Circuit: Jurnal Ilmiah Pendidikan Teknik Elektro
Volume 8 No. 2 March 2024 - August 2024
ISSN: 2549-3698; E-ISSN: 2549-3701
DOI: 10.22373/crc.v8i2.22091

Power Deficit Analysis of Multiple Hydrokinetic Power Plants in an Open-Channel System

Muhammad Ikhsan[a,b], Zufrizal[a], Taufik[a]

[a] Universitas Islam Negeri Ar-Raniry Banda Aceh, Indonesia

[a,b] Institute of Control Systems, RPTU Kaiserslautern-Landau, Germany

E-mail: m.ikhsan@ar-raniry.ac.id; https://eit.rptu.de/en/lrs/staff

Submission: 10-01-2024 Accepted: 05-06-2024 Published: 12-07-2024

Abstract

The electricity generation capacity of hydrokinetic power plants can be enhanced by paralleling multiple plants simultaneously. This study focuses on the longitudinal configuration of multiple hydrokinetic turbines installed in a water channel. The energy production rate of downstream turbines is lower than that of upstream turbines when placed close to each other. This observed phenomenon, related to the wake effect, has resulted in reduced flow velocity. In this research, a power deficit technique is employed as an alternative to the velocity deficit strategy. By estimating the open flow characteristic, or k, this method aims to predict the downstream power input at any given time. Without directly measuring water velocity, power can be predicted using the power deficit model. A hybrid model combining the Bastankhah Porté-Agel model and the Geometry-Based model has been utilized in this study. The analysis results indicate that the power deficit and velocity deficit values differ by an average of 1.3% and 0.15%, respectively.*

Keywords*: Hydrokinetic, Bastankhah Porté-Agel model, Geometry-Based model*

Abstrak

Kapasitas generasi listrik dari pembangkit listrik hidrokinetik dapat ditingkatkan dengan cara memparalel banyak pembangkit secara bersamaan. Konfigurasi longitudinal dari banyak turbin hidrokinetik yang dipasang di saluran air adalah subjek penelitian ini. Tingkat produksi energi turbin *downstream* lebih rendah daripada turbin *upstream* ketika ditempatkan dekat satu sama lain. Fenomena yang telah terlihat terkait dengan efek alarm, telah mengurangi kecepatan aliran. Sebuah teknik defisit daya digunakan sebagai alternatif untuk strategi defisit kecepatan dalam penelitian ini. Dengan memperkirakan karakteristik aliran terbuka, atau k*, metode ini bertujuan untuk memprediksi input daya *downstream* pada saat tertentu dalam waktu. Tanpa benar-benar mengukur kecepatan air, daya dapat diprediksi dengan menggunakan model defisit daya. Sebuah model hibrida yang menggabungkan model *Bastankhah Porté-Agel* dan model *Geometry-Based* telah digunakan dalam penelitian ini. Hasil analisis menunjukkan bahwa nilai defisit daya dan nilai defisit kecepatan berbeda rata-rata 1,3% dan 0,15%, masing-masing.

Kata kunci: Hidrokinetik, model Bastankhah Porté-Agel, Model Geometri

Introduction

Hydrokinetic power plant development has attracted a lot of interest from diverse stakeholders, covering not only scholars but also governmental entities [1, 2]. The generation of energy in a hydrokinetic power plant is solely dependent on the utilization of the kinetic energy present in the movement of water [3, 4, 5]. The technology described in the literature is not limited only to river flows, but can also be applied to ocean currents [6, 7] or irrigation flows [8]. Hydrokinetic power plants exhibit the advantage of not necessitating extensive dam construction or civil infrastructure, thereby reducing associated costs [9] and environmental impacts [10]. Furthermore, these power plants offer relatively rapid installation periods [11] and do less impede the natural flow of water [12], thereby minimizing potential disruptions to aquatic ecosystems. The implementation of this particular generator within the river ecosystem will not induce any modifications to the established patterns of fish migration [13] nor interfere with the natural flow of sedimentation within the watercourse.

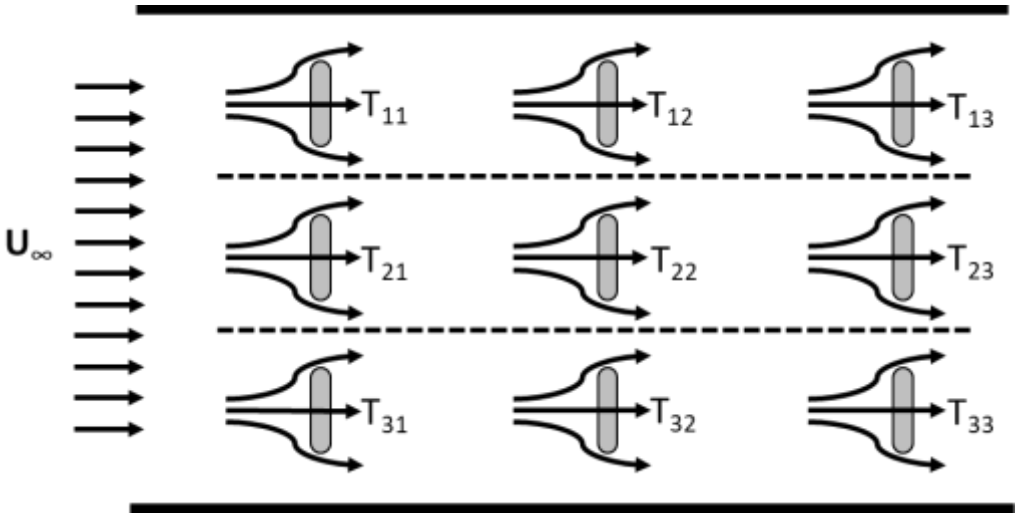

Figure 1. Layout of a Hydrokinetic Power Plant

Multiple hydrokinetic power plants can be operated simultaneously in order to enhance the capacity for power generation. Although the flow of water is less fluctuating compared to wind, the location of the turbine needs to be planned so that the system works more efficiently [14]. The power plant has the capability to be installed in three different configurations: transverse [15], longitudinal [16], or a combination of both [17], as depicted in Figure 1. Large areas, such as the seabed, can be subjected to one or a combination of two placement methods. However, in order to mitigate power losses caused by boundary effects [18] or accommodate the restricted width of waterways [19], it is beneficial to choose a longitudinal laying approach, particularly in areas with relatively narrow flows, such as rivers, water canals, or irrigation [20].

The installation of a hydrokinetic power plant in a longitudinal orientation on an irrigation canal offers numerous benefits. These benefits include taking advantage of the pre-existing canal structure and the possibility of installing the power plant alongside the irrigation canal. Nonetheless, the longitudinal installation of the hydrokinetic turbine may result in the generation of a wake effect, leading to a decrease in the kinetic energy of the water [21]. Consequently, this reduction in energy can have an adverse impact on

the power output of the downstream power plant, contributing to a power deficit. Further analysis is required to investigate the power deficit resulting from the wake effect. This analysis aims to optimize the energy production of each hydrokinetic power plant installed in a longitudinal configuration.

The study examines the electric power deficit in hydrokinetic power plants situated in open channels with a longitudinal configuration, employing the wake effect theory. The goal of this study is to develop a novel wake effect model based on power deficit. The objective is to ensure that hydrokinetic power generators with longitudinal configurations can operate stably and optimally without requiring direct water velocity measurements using sensors. By employing the power deficit approach, changes in input power for downstream turbines due to flow fluctuations can still be predicted. This model has the potential to enhance the efficiency and performance of hydrokinetic power plants. The validation of the wake effect model is conducted using software based on Computational Fluid Dynamics (CFD). The first part presents a correlation model that examines the relationship between the wake effect and the power deficit. This model will be constructed by integrating both Geometry-Based model (GM) and Bastankhah Porté-Agel model (BPA). In the next part, the model is verified through CFD analysis. The obtained model can be subsequently utilized in the control implementation of multiple hydrokinetic array power plants.

Literature Review

a. Kinetic Energy of Water Flow

Hydrokinetic power plants do not require the potential energy of water but only require kinetic energy, which satisfies equation (1):

$$P_t = \frac{1}{2} C_p \rho A V^3 \quad \text{.....} \quad (1)$$

Where Cp is the power coefficient, ρ is the density of the fluid (water = 998 kg/m3), A is the sweep area of the turbine blades (m2), and V is the velocity of the fluid flow (m/s). In addition to employing a turbine with a large swept area and an extra water flow velocity, the capacity for power generation can be enhanced through the parallelization of multiple generation units within a power grid [22].

b. Wake Effect

The previously mentioned idea of installing turbines in longitudinal will certainly have an impact on other turbines that rely on the same water flow. The primary (upstream) turbine will induce turbulence in the fluid stream [23]. When turbines are positioned in close proximity to one another, the downstream turbines will generate electricity at a lower rate than the upstream turbines [24]. This phenomenon is commonly referred to as the wake effect.

c. Bastankhah Porté-Agel Model

The mathematical representation of wake effects can be achieved through the utilization of the BPA model, as proposed in [25]. This model enables the observation of the point at which the wake effect ends to be apparent. According to the BPA, the

reduction in water flow velocity caused by the wake effect is assumed to follow a Gaussian distribution, as described by the equation (2).

$$\frac{\Delta U}{U_\infty} = C(x)\, e^{-\frac{r^2}{2\sigma^2}} \quad \text{..... (2)}$$

Where ΔU/U∞ is the water velocity deficit, r is the turbine radius. C(x) and σ can be described as equations (3)

$$\frac{\Delta U}{U_\infty} = \left(1 - \sqrt{\frac{C_T}{8\left(k^*\frac{x}{d_0}+0.2\sqrt{\beta}\right)^2}}\right) \times exp\left(-\frac{1}{2\left(k^*\frac{x}{d_0}+0.2\sqrt{\beta}\right)^2}\left\{\left(\frac{z-z_h}{d_0}\right)^2 + \left(\frac{y}{d_0}\right)^2\right\}\right) \quad \text{..... (3)}$$

The parameter k* represents the rate at which the wake effect is able to recover. This parameter is highly influenced by the physical attributes of the river or irrigation system, such as the coefficient of friction and the canal shape. The representation of β can be expressed in accordance with (4), where CT is the thrust coefficient.

$$\beta = \frac{1+\sqrt{1-C_T}}{2\sqrt{1-C_T}} \quad \text{..... (4)}$$

d. Geometry-Based Model

The application of the Geometry-Based model in wake analysis allows the estimation of the power deficit of a hydrokinetic turbine. Empirical coefficients and linear regression analysis are both used in this model [26]. Two crucial variables in this model are the blockade ratio BR_i, which satisfies the condition $0 \leq BR_i \leq 1$, and the blockage distance BD_i. Both expressions can be represented mathematically as (5) and (6).

$$BR_i = \frac{1}{A}\int_A xdA \quad \text{..... (5)}$$

$$BD_i = \frac{1}{A}\int_A LxdA \quad \text{..... (6)}$$

Relative power can be written directly as (7)

$$P_i^{Rel} = \frac{P_i}{P_u}\begin{cases}\alpha + \beta BR_i + \frac{\gamma BD_i}{L_\infty} & BR_i \geq 0 \\ 1 & BR_i = 0\end{cases} \quad \text{..... (7)}$$

Method

The theoretical framework employed in this study is derived from a synthesis of various foundational works related to the phenomenon of wake effects. The research flowchart is visually illustrated in Figure 2.

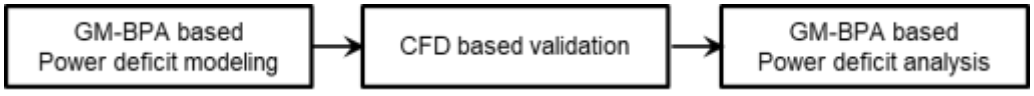

Figure 2. The Research Flowchart

The formulation of power deficit modeling is based on the integration of two wake effect concepts, particularly the GM and the BPA model. It is assumed that hydrokinetic turbines are operating at their respective maximum power points and

arranged in a longitudinal manner within water canals, such as those used for irrigation, as shown in Figure 3. T_1 represents a turbine located upstream, whereas T_2 and T_3 denote turbines situated downstream. L_{mn} represents the distance between the turbines. According to the Geometry-Based model, the blocking ratio BR of T_1 is determined to be zero, whereas the blocking ratio of T_2 and T_3 is found to be 1, indicating complete blocking.

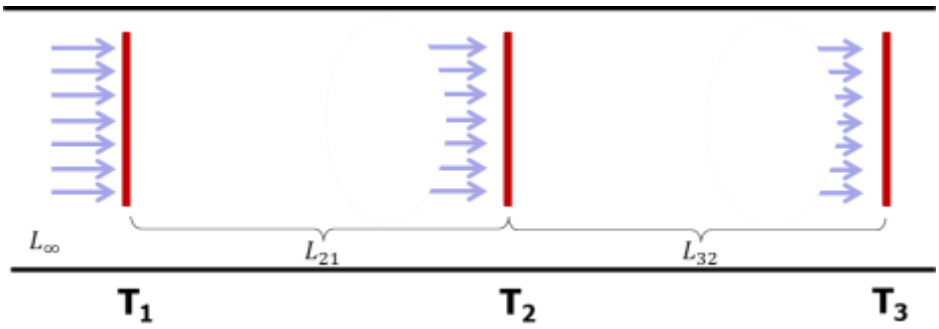

Figure 3. System Assumptions

$$BR_1 = 0 \quad \ldots\ldots\ldots\ldots\ldots\ldots\ldots\ldots\ldots\ldots\ldots\ldots\ldots\ldots\ldots\ldots\ldots\ldots \quad (8)$$

$$BR_2 = BR_3 = 1 \quad \ldots\ldots\ldots\ldots\ldots\ldots\ldots\ldots\ldots\ldots\ldots\ldots\ldots\ldots\ldots\ldots\ldots\ldots \quad (9)$$

Based on (7) the relative power equation of each turbine can be simplified into (10)-(12),

$$P_1^{REL} = \alpha_1 + \gamma_1 BD_1/L_\infty \quad \ldots\ldots\ldots\ldots\ldots\ldots\ldots\ldots\ldots\ldots\ldots\ldots\ldots\ldots\ldots\ldots\ldots\ldots \quad (10)$$

$$P_2^{REL} = \alpha_2 + \gamma_2 BD_2/L_{21} \quad \ldots\ldots\ldots\ldots\ldots\ldots\ldots\ldots\ldots\ldots\ldots\ldots\ldots\ldots\ldots\ldots\ldots\ldots \quad (11)$$

$$P_3^{REL} = \alpha_3 + \gamma_3 BD_3/L_{32} \quad \ldots\ldots\ldots\ldots\ldots\ldots\ldots\ldots\ldots\ldots\ldots\ldots\ldots\ldots\ldots\ldots\ldots\ldots \quad (12)$$

Then,

$$P_{front} = P_1 = 1 \quad \ldots\ldots\ldots\ldots\ldots\ldots\ldots\ldots\ldots\ldots\ldots\ldots\ldots\ldots\ldots\ldots\ldots\ldots \quad (13)$$

$$P_2 = (\alpha_2 + \gamma_2 BD_2/L_{21})P_1 \quad \ldots\ldots\ldots\ldots\ldots\ldots\ldots\ldots\ldots\ldots\ldots\ldots\ldots\ldots\ldots\ldots\ldots\ldots \quad (14)$$

$$P_3 = (\alpha_3 + \gamma_3 BD_3/L_{32})P_2 \quad \ldots\ldots\ldots\ldots\ldots\ldots\ldots\ldots\ldots\ldots\ldots\ldots\ldots\ldots\ldots\ldots\ldots\ldots \quad (15)$$

Consider C_{BDn} as relative power coeficient between upstream to downstream turbine, we can rewrite is as (16)

$$\frac{P_2}{P_1} = C_{BD_2} \quad \ldots\ldots\ldots\ldots\ldots\ldots\ldots\ldots\ldots\ldots\ldots\ldots\ldots\ldots\ldots\ldots\ldots\ldots \quad (16)$$

Referring back to (1) and substituting it with (16), The equation can be written as (17)

$$\frac{P_2}{P_1} = \frac{0.5\rho AC_{p2}V_2^3}{0.5\rho AC_{p1}V_1^3} \quad \ldots\ldots\ldots\ldots\ldots\ldots\ldots\ldots\ldots\ldots\ldots\ldots\ldots\ldots\ldots\ldots\ldots\ldots \quad (17)$$

In the scenario where all turbines have identical parameters and operate at the same coefficient of performance CP, such as when employing maximum power point tracking (MPPT), then $C_{p1} \approx C_{p2}$, thus,

$$\frac{P_2}{P_1} = \frac{V_2^3}{V_1^3} \quad \text{(18)}$$

substitute with (16), then

$$\frac{V_2}{V_1} = \sqrt[3]{C_{BD_2}} \quad \text{(19)}$$

The velocity deficit definition can be written as (20),

$$\frac{\Delta U}{U_\infty} = 1 - \frac{U_w}{U_\infty} \quad \text{(20)}$$

The upstream velocity U_∞ is considered equal to the stream velocity on the upstream turbine V1, and the wake velocity UW is equal to the stream velocity on the downstream turbine V2. Substituting (20) with (19) then the relation of velocity deficit and power deficit during maximum operation of each turbine can be written to (21)

$$\frac{\Delta U}{U_\infty} = 1 - \sqrt[3]{C_{BD_2}} \quad \text{(21)}$$

The thrust coefficient (C_T) will be 0.88 If the Cp is at its maximum value. When the electric power measurement of each turbine is available, the stream "characteristic" k* can be calculated. Moreover, the stream velocity can be estimated from the turbine's output power indirectly without the use of a water current sensor. This is the benefits of the power deficit model of (21).

The validation process was conducted using Ansys Fluent software by comparing the power deficit model to the velocity deficit model. The longitudinal separation between the upstream and downstream turbines in the water channel is 10 meters. Due to licensing limitations, only two turbines were employed in validating the GM-BPA model. The open channel is 2.5 meters deep and 6 meters wide. The stream is assumed to have a velocity of up to 3 m/s, and it has a base roughness level of 1mm. The validation configuration is shown in Figure 4. While there is no obligation to use a specific turbine model, it is crucial to emphasize that all turbines employed must be of the same type. The hydrokinetic turbine model has been constructed according to the reference [27].

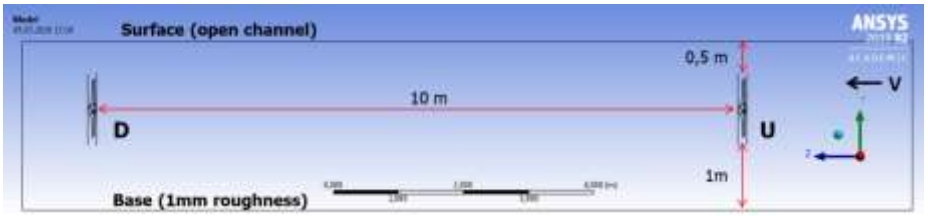

Figure 4. Validation Setup

In order to determine the turbine's maximum operating point, the water velocity at the inlet is gradually adjusted within the range of 1 to 3 m/s. During these conditions, the torque of the turbine is consistently measured. The turbine set rotates at a specific RPM, steadily increasing until reaching the maximum torque value. This specific operating point is then designated as the turbine's maximum working point. The simulation configuration can be seen according to Table 1.

Table 1. Simulation Setup

Simulation Parameter	Setting
Domain enclosure	Water: 1 atm reference pressure, stationary
Boundary condition	Medium turbulence (intensity=5%)
	flow regime: Subsonic
Boundary type	Inlet: normal speed 1-3 m/s
	Outlet: opening
	Bottom side (base): rough wall with 1 mm roughness
	Top side (surface): opening
	Left/right side: rough wall with 1 mm roughness
Mesh setup	Mesh Elements: 1.650.911
	Mesh Nodes: 356.093
	Reference Pressure: 1 atm
Turbulence	Model: k-epsilon
	Turbulent Wall Functions: Scalable
Buoyancy model	Non Buoyant
Turbine	Blade diameter: 1m
	Blade number: 3
Solver setting	Advection scheme: High Resolution
	Turbulence numeric: High Resolution
	Max. Iteration: 10000
	Timescale: auto, conservative
	Timescale factor: 1.0
	Residual type: RMS
	Residual target: 1.E-4

Result and Discussion

Both turbines are designed to harness energy at their respective maximum operating conditions, leading to identical values for the coefficient of performance C_{p1} and C_{p2}. The desired outcome is attained through the manipulation of the angular velocity while simultaneously monitoring the amount of power generated by the turbine. The simulation was conducted five times, each time using different flow velocities that ranged from 1 to 5 m/s. The findings regarding the measurement of the maximum power and angular speed are presented in Table 2.

Table 2. The Turbine's Maximum Power Output at the Corresponding Angular Velocity

V (m/s)	Max Power (W)		Ang. Velocity (RPM)	
	U	D	U	D
3.0	3204.03	3023.13	-70	-69
2.5	1842.77	1602.91	-57	-56
2.0	943.808	703.274	-46	-44
1.5	396.097	200.866	-34	-32
1.0	116.239	2.38716	-23	-20

The simulation results additionally show the development of a wake effect resulting from the presence of the upstream turbine, as illustrated in Figure 5. The stream velocity behind the upstream turbine is measured every 1 meter. The data shown in Figure 6 indicates a reduction in the flow velocity, yet with a gradual recovery. The

decrease in flow velocity occurs again when the water approaches the downstream turbine; this phenomenon is known as the blockage effect.

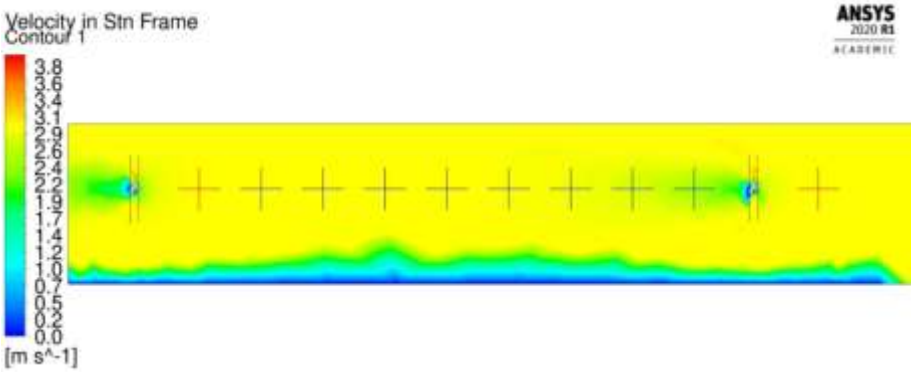

Figure 5. The Wake Effect the Development in Open Channel Flow

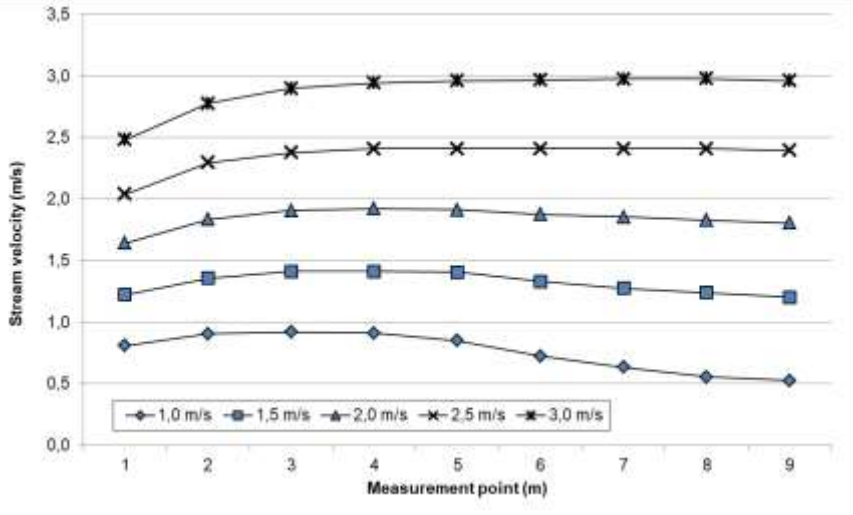

Figure 6. The Measuring Results of Stream Velocity Every 1 Meter After the Upstream Turbine

a. The Comparison Between Velocity Deficit and Power Deficit

To determine the value of the velocity deficit, it is necessary to measure the flow speed, either by employing a current meter or an alternative velocity sensor. To determine the power deficit value, in the case of a power generation system, it is necessary to measure the power on the generator terminal. Table 3 shows a comparison of measurements based on velocity deficit and power deficit for variations in water speed of 1 to 3 m/s. The measurement of velocity deficit is conducted in accordance with Figure 5, specifically at the locations indicated by the red cross markers. In order to perform power deficit calculation, the power measurement data from individual turbines can conveniently be extracted directly from Ansys. Subsequently, equation (20) is employed to acquire the data presented in Table 3. Visually, this can be observed in the graphical representation depicted in Figure 7.

Table 3. Comparison Between Velocity Deficit and Power Deficit Measurement

V Input (m/s)	Vel. Deficit	Pow. Deficit	Δ (%)
1.0	0.4553	0.7262	**27.09**
1.5	0.1799	0.2026	2.26

2.0	0.0829	0.0934	1.05
2.5	0.0380	0.0454	0.74
3.0	0.0072	0.0192	1.20

It can be seen that both deficits have significant differences, especially at low stream velocities. The reason behind this phenomenon lies in the fact that the downstream turbine's performance may be compromised when operating at lower flow velocities. As a result, the downstream turbine is unable to extract a significant amount of energy, which causes the system to experience a major power deficit.

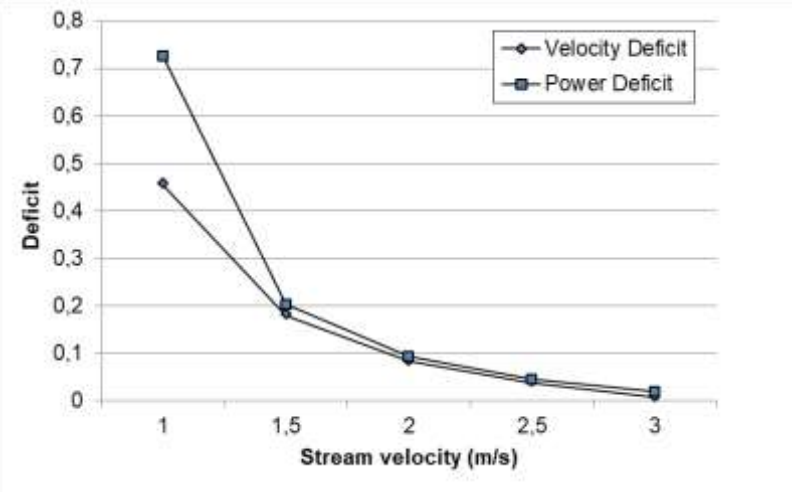

Figure 7. Velocity Deficit and Power Deficit Measurement

b. Calculation of k*

In the BPA model, the value of k* will have an impact on how quickly the wake effect recovers. The greater the value, the faster the wake effect recovers. There is no best value for this k* value, and each open channel will have its own k* value. This value may be analogous to flow characteristics, which depend on channel dimensions, fluid velocity, and the level of turbulence that occurs.

Table 4. Calculation of k* after 9 m

V Input (m/s)	k* Calculation		Δ (%)
	With Vel. Deficit	With Pow. Deficit	
1.0	0.1485	0.1923	**29.5068**
1.5	0.1344	0.1350	0.4517
2.0	0.1326	0.1328	0.0933
2.5	0.1323	0.1323	0.0309
3.0	0.1322	0.1322	0.0158

Back to (3), k* can be determined if the velocity deficit (or power deficit) is already known. The k* value in this study is calculated at a distance of 9 meters behind the upstream turbine. Given the assumption that the turbines are operating at their maximum efficiency, Table 4 displays the computed values of k* when measured at a distance of 9 meters. In addition, this study also provides a comparison of k* calculations based on velocity deficit. The table additionally illustrates that the value of k* for a given open channel will vary depending on its flow velocity. The k* value for

velocities below 1.5 m/s once again exhibits a significant difference in comparison to the velocities above it.

Conclusion

In this study, the Geometry-Based model and the BPA model are combined to form the GM-BPA model, which is then simplified by assuming that each upstream and downstream turbine operates at its peak efficiency. The model derived in this study was subjected to multiple validations using Ansys software, employing several stream velocity values. According to the validation results, for flow velocities greater than 1.5 m/s, there is an average difference of 1.3% between the power deficit value and the velocity deficit value. At lower flow velocities, a notable disparity exists between the two. The neglect of this aspect is justified due to the limited application of hydrokinetic turbines in scenarios involving low stream velocities.

The GM-BPA model, which is based on the power deficit concept, can be utilized to estimate open flow characteristics by using k* values. During stream velocity under 1.5 m/s, there is an observed variation in the value of k* between power deficit-based GM-BPA and velocity deficit-based BPA, with an average difference of 0.15%. The power deficit model can also be employed for the purpose of forecasting the power that will be acquired by a hydrokinetic turbine located downstream at a specific time, as a consequence of fluctuations in stream velocity. The task can be accomplished without requiring the direct measurement of water flow velocity. Further studies are required concerning the implementation of the proposed GA-BPA model in the context of cooperative control of hydrokinetic turbine circuits and predictive control.

Acknowledgement

The authors express their gratitude to the Ministry of Religion of the Republic of Indonesia for providing financial support [Grant numbers 397/PPK-UIN/PUSLIT/II/2023].

References

[1] M. I. Ibrahim and M. J. Legaz, “Hydrokinetic power potential in Spanish coasts using a novel turbine design,” *J. Mar. Sci. Eng.*, vol. 11, no. 5, p. 942, 2023. https://doi.org/10.3390/jmse11050942

[2] M. Ikhsan and M. R. Fachri, “Power control study of hydrokinetic power plants in presence of wake effect,” *Circuit: Jurnal Ilmiah Pendidikan Teknik Elektro*, vol. 7, no. 1, p. 47, 2023. http://dx.doi.org/10.22373/crc.v7i1.14650

[3] K. Kirby, C. D. Rennie, J. Cousineau, S. Ferguson, and I. Nistor, “Impacts of seasonal flow variation on riverine hydrokinetic energy resources and optimal turbine location – Case study on the Rivière Rouge, Québec, Canada,” *Renew. Energy*, vol. 210, pp. 364–374, 2023. https://doi.org/10.1016/j.renene.2023.04.067

[4] W. I. Ibrahim, M. R. Mohamed, R. M. T. R. Ismail, P. K. Leung, W. W. Xing, and A. A. Shah, “Hydrokinetic energy harnessing technologies: A review,” *Energy Rep.*, vol. 7, pp. 2021–2042, 2021. https://doi.org/10.1016/j.egyr.2021.04.003

[5] Zufrizal, M. Ikhsan and G. I. Yasaa, "Assessment of the Kluet River's Potential for

Hydrokinetic Power Generation," International Conference On Vocational Education, Electrical & Electronic Engineering, vol. 1, no. 1, 2024.

[6] I. Iglesias, A. Bio, L. Bastos, and P. Avilez-Valente, "Estuarine hydrodynamic patterns and hydrokinetic energy production: The Douro estuary case study," *Energy (Oxf.)*, vol. 222, no. 119972, p. 119972, 2021. https://doi.org/10.1016/j.energy.2021.119972

[7] C. M. Niebuhr, M. van Dijk, V. S. Neary, and J. N. Bhagwan, "A review of hydrokinetic turbines and enhancement techniques for canal installations: Technology, applicability and potential," *Renew. Sustain. Energy Rev.*, vol. 113, no. 109240, p. 109240, 2019. https://doi.org/10.1016/j.rser.2019.06.047

[8] I. Khan *et al.*, "Analysis of Jamrao canal for potential of hybrid photovoltaic/hydrokinetic turbine system," *Energy Rep.*, vol. 10, pp. 419–430, 2023. https://doi.org/10.1016/j.egyr.2023.06.052

[9] O. A. S. Olatunji, A. T. Raphael, and I. T. Yomi, "Hydrokinetic Energy Opportunity for Rural Electrification in Nigeria," *Int. J. Renew. Energy Dev.*, vol. 7, no. 2, pp. 183–190, 2018. https://doi.org/10.14710/ijred.7.2.183-190

[10] D. M. Fouz, R. Carballo, I. López, and G. Iglesias, "A holistic methodology for hydrokinetic energy site selection," *Appl. Energy*, vol. 317, no. 119155, p. 119155, 2022. https://doi.org/10.1016/j.apenergy.2022.119155

[11] M. J. Khan, M. T. Iqbal, and J. E. Quaicoe, "River current energy conversion systems: Progress, prospects and challenges," *Renew. Sustain. Energy Rev.*, vol. 12, no. 8, pp. 2177–2193, 2008. https://doi.org/10.1016/j.rser.2007.04.016

[12] A. R. Badger, "Technology assessment of hydrokinetic energy: Run-of-river and in-stream tidal systems," James Madison University, 2011. https://commons.lib.jmu.edu/master201019/141

[13] E. Brown, S. Sulaeman, R. Quispe-Abad, N. Müller, and E. Moran, "Safe passage for fish: The case for in-stream turbines," *Renew. Sustain. Energy Rev.*, vol. 173, no. 113034, p. 113034, 2023. https://doi.org/10.1016/j.rser.2022.113034

[14] M. Ikhsan, A. Purwadi, N. Hariyanto, N. Heryana, and Y. Haroen, "Study of renewable energy sources capacity and loading using data logger for sizing of solar-wind hybrid power system," *Procedia Technol.*, vol. 11, pp. 1048–1053, 2013. https://doi.org/10.1016/j.protcy.2013.12.293

[15] L. Cacciali, L. Battisti, and S. Dell'Anna, "Multi-array design for hydrokinetic turbines in hydropower canals," *Energies*, vol. 16, no. 5, p. 2279, 2023. https://doi.org/10.3390/en16052279

[16] B. Gunawan, V. Neary, J. Mortensen, and J. Roberts, "Assessing and testing hydrokinetic turbine performance and effects on open channel hydrodynamics: An irrigation canal case study," Office of Scientific and Technical Information (OSTI), 2017. https://doi.org/10.2172/1367421

[17] O. Pacot, D. Pettinaroli, J. Decaix, and C. Münch-Alligné, "Cost-effective CFD simulation to predict the performance of a hydrokinetic turbine farm," *IOP Conf. Ser. Earth Environ. Sci.*, vol. 405, no. 1, p. 012037, 2019. https://doi.org/10.1088/1755-1315/405/1/012037

[18] N. Kolekar and A. Banerjee, "Performance characterization and placement of a marine hydrokinetic turbine in a tidal channel under boundary proximity and blockage effects," *Appl. Energy*, vol. 148, pp. 121–133, 2015. https://doi.org/10.1016/j.apenergy.2015.03.052

[19] G. Giannini, V. Ramos, P. Rosa-Santos, T. Calheiros-Cabral, and F. Taveira-Pinto, "Hydrokinetic power resource assessment in a combined estuarine and river region," *Sustainability*, vol. 14, no. 5, p. 2606, 2022.

https://doi.org/10.3390/su14052606

[20] M. Sood and S. K. Singal, "A numerical analysis to determine wake recovery distance for the longitudinal arrangement of hydrokinetic turbine in the channel system," *Energy Sources Recovery Util. Environ. Eff.*, pp. 1–22, 2021. https://doi.org/10.1080/15567036.2021.1979695

[21] I. F. S. dos Santos, R. G. R. Camacho, and G. L. Tiago Filho, "Study of the wake characteristics and turbines configuration of a hydrokinetic farm in an Amazonian river using experimental data and CFD tools," *J. Clean. Prod.*, vol. 299, no. 126881, p. 126881, 2021. https://doi.org/10.1016/j.jclepro.2021.126881

[22] N. Narayanan K. and L. Umanand, "Parallel operation of doubly fed induction generators and inverters in a microgrid," in *2020 IEEE International Conference on Power Electronics, Smart Grid and Renewable Energy (PESGRE2020)*, 2020. https://doi.org/10.1109/PESGRE45664.2020.9070744

[23] M. Guerra and J. Thomson, "Wake measurements from a hydrokinetic river turbine," *Renew. Energy*, vol. 139, pp. 483–495, 2019. https://doi.org/10.1016/j.renene.2019.02.052

[24] M. F. Howland, S. K. Lele, and J. O. Dabiri, "Wind farm power optimization through wake steering," *Proc. Natl. Acad. Sci. U. S. A.*, vol. 116, no. 29, pp. 14495–14500, 2019. https://doi.org/10.1073/pnas.1903680116

[25] M. Bastankhah and F. Porté-Agel, "A new analytical model for wind-turbine wakes," *Renew. Energy*, vol. 70, pp. 116–123, 2014. https://doi.org/10.1016/j.renene.2014.01.002

[26] N. S. Ghaisas and C. L. Archer, "Geometry-based models for studying the effects of wind farm layout," *J. Atmos. Ocean. Technol.*, vol. 33, no. 3, pp. 481–501, 2016. https://doi.org/10.1175/jtech-d-14-00199.1

[27] "Free CAD designs, files & 3D models," *Grabcad.com*. [Online]. Available: https://grabcad.com/library/hydrokinetic-turbine. [Accessed: 10-Jan-2024].